Hanging wall deformation in the Western Rift

Dan Sandiford(1), Sascha Brune(2), Anne Glerum(2), John Naliboff(3)

1: University of Tasmania, 2: GFZ Potsdam, 3: New Mexico Tech University

Study overview

- In strongly asymmetric (half graben) segments of the western rift (WR), the kinematics induced by border fault slip are likely to play a major role in the deformation of hangingwall blocks.
- While near surface faulting patterns in hangingwall blocks are becoming increasingly well resolved, the relative contribution of flexural strain, space accommodation (hanging wall collapse) and bulk extension (migration of extension from border faults) is not well understood.

Key questions

- What modes of deformation contribute to hanging wall deformation in the WR half grabens?
- What do border and intrarift faults do in the lower crust, and how is deformation partitioned into the mantle lithosphere.
- Can patterns of hangingwall faulting place constraints on the lithosphere mechanics - for instance on the relative strength of the mantle lithosphere.

Structural character of western rift basins

- The typical basin width and border fault length of WR basins, suggest that brittle deformation dominates to moho depths of 35 - 40 km, consistent with earthquake hypocenter depths.
- Basin profiles are often highly asymmetric (half graben), where total extensions of around 4-10 km have mainly been accommodated on border faults.
- Border fault escarpments evidence about 1-2 km of upfift, as predicted by models of regional isostatic uplift around a major normal fault [5].
- Hangingwalls basement shows an overall downwarping, with depocenters adjacent to border faults, and sediment thicknesses reaching up to 8 km.
- Geological and seismic studies reveal that significant faulting has developed in many basin hangingwalls, with throws of up to 2 kilometers [4].
- In a number of highly asymmetric basin segments, hangingwall faults exhibit a dip domain synthetic to the border faults, with spacing and fault throw generally decreasing away from the border (e.g. North Basin, Malawi, see Figures below).

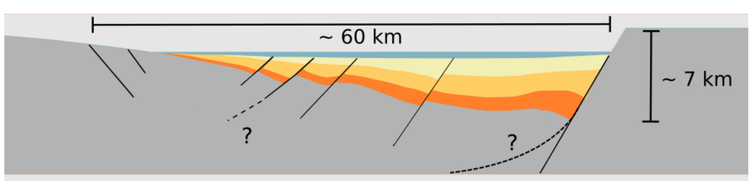

Schematic of a WR basin (half graben). Figure adapted from Wright et al. [6]. Lengths are representative of general features of the western rift.

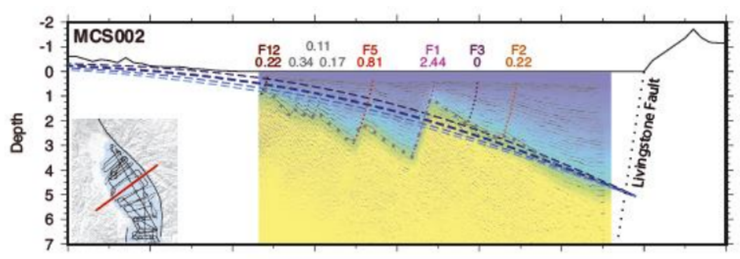

Seismic refelction image across the North Basin of the Malawi Rift, from Shillington et al. [4]. Total horizontal distance shown is 80 km.

Modelling approach and validation

Models are built with the ASPECT code [1], a parallel finite element solver for the Stokes equations. The lithosphere is modelled as an incompressible Maxwell visco-elastic-plastic (VEP) material, following the approach of [2].

Following the numerical investigation of Arthur-Olive et al. [3], we begin by simulating the elastic flexural-isostatic response of the lithosphere to deformation along a single throughgoing planar fault. This model has a strong similarity the semi-analytic model of Weissel and Karner [5, 3], although the assumption that the fault is welded (subsequent to slip) is not valid here. Nevertheless, we find that the deformation, particularly the flexural uplift of the footwall closely approximates the flexural-isostatic model.

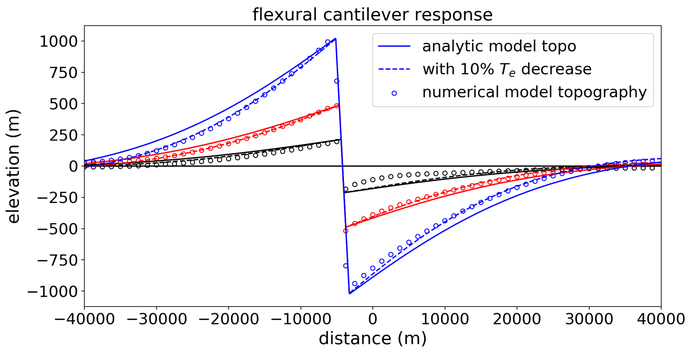

M1: single layer - planar fault

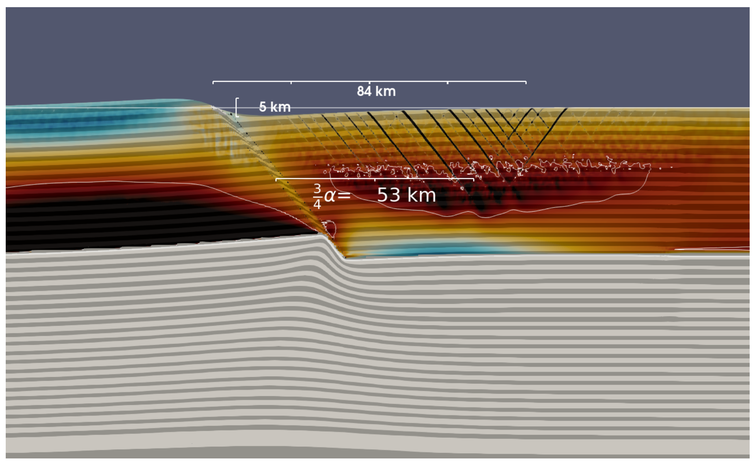

M1 shown at total extension of 8 km. The basin width, as measured by the distance from border fault to first prominent conjugate fault is ~ 80 km. Black lines show plastic strain, white line shows 100 MPa contour of the σ_{xx} component of the deviatoric stress. Faulting in the hangingwall is mainly sythetic to the border fault. The maximum deformation on these synthetic faults is estimated to be around hundred meters. The predicted maximum curvature in the flexural-isostatic loading model of Weissel and Karner [5] is approximately $\frac{3}{4}\alpha$, where α is the flexural parameter. This region, shown in the Figure, coincides with the highest stresses, and most intense brittle flexural deformation of the hangingwall.

M2: single layer - listric fault

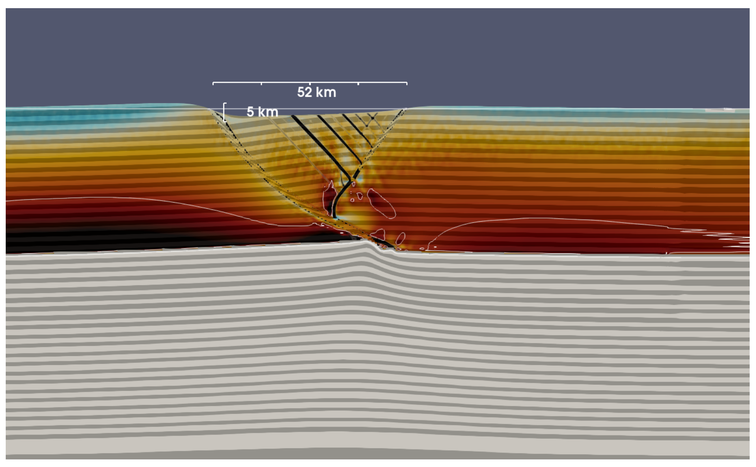

M2 shown at total extension of 8 km. The hanging wall faulting pattern consists of a prominent conjugate fault rooted to the border fault, and a set of synthetic faults within basin. This pattern emerges at extensions of about 4 km (half those shown here). Maximum slip on the synthetic hangingwall faults is estimated to be about 1 km. We note that a similar model (not shown), except with a 10 km strong mantle layer coupled to the crust, produced similar patterns of crustal faulting.

M3: three layer - planar fault

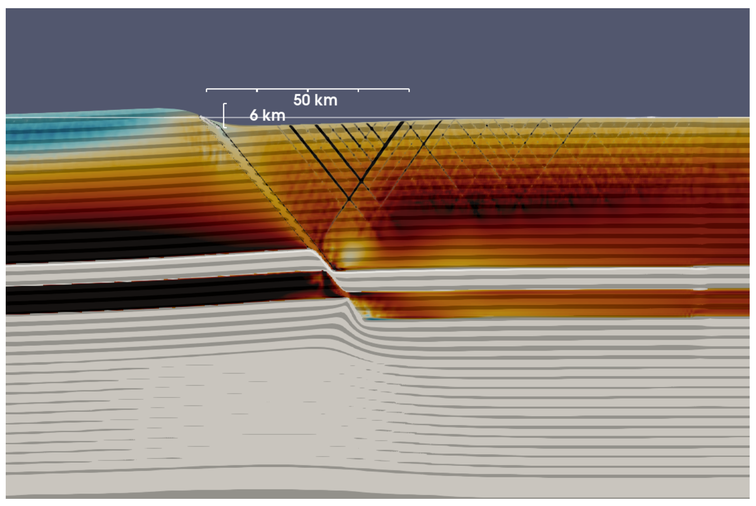

M3 shown at total extension of 8 km. The model setup differs to M1 in that a strong mantle lithosphere layer is added, and decoupled from the brittle crust via a 5 km thick ductile layer (presumed to be the lowermost crust). In this setup a prominent conjugate fault develops, rooting at the brittle/ductile transition in the crust. A synthetic (WRT to the border fault) dip domain develops within the basin, rooting onto the main conjugate fault. The deformation on these synthetic faults is estimated to be less than a few hundred meters, significantly less than in the listric fault model (M2).

Acknowledgments

We thank the Computational Infrastructure for Geodynamics (http://geodynamics.org) which is funded by the National Science Foundation under awards EAR-0949446 and EAR-1550901.

This research was funded by the Australian Government through the Australian Research Council.

single layer model setup

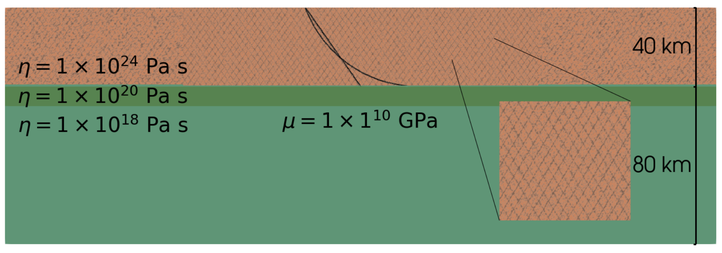

single brittle layer model setup

The 2d models have constant velocity boundary conditions applied to the sidewalls, with a full extension rate of 0.4 cm/y, and uniform compensating flow through the lower boundary. The surface is tractionless, except for some stability terms. A surface slope diffusion scheme is used to avoid excessive deformation of the mesh. The brittle yield stress follows the Drucker-Prager criterion. Shear band localisation is driven by strain weakening of the cohesion and friction angle (20 MPa, 20 °), which both weaken to 20 percent of their value over a strain interval of 1. The model is initialised with both random plastic strain as well as a 'fabric' oriented at the optimal (Coulomb) angles, as shown in the Figure inset. The main border faults are initialised with a strain of 1 (fully weakened) in either a planar or listric geometry as shown.

Discussion

- The hangingwall deformation observed in WR half grabens is inconsistent with flexure of a single 40 km thick elasto-brittle layer, even when pervasive brittle weakening (and loss of flexural rigidity) is modelled. Models where hangingwall deformation is dominated by flexure (e.g. M1) develop typical fault offsets on the order of 100s meters, whereas they reach several kilometers in some WR cases [4]; Moreover, the width of the basins developed in M1, exceeds the typical width of WR basins.
- A model with a listric border fault and a prominent conjugate fault that roots near the base of the brittle layer, provides intrarift faulting patterns that reconcile better with observations. These models show intrarift fault offsets of around a kilometer, and basin around 50 km, within the typical WR range.
- Conjugate faults that root onto the border fault develop in a variety of models. The single brittle layer with listric border fault is one example. A conjugate fault also develops in three layer model, with a strong brittle mantle layer, decoupled by a presumed thin ductile zone in the lowermost crust.
- At total extension (heave) lengths of 8 km, models predict basement subsidence, relative the initial surface, of around 3 - 4 km. None of the models produce enough basement subsidence to accommodate sediment thicknesses (6 - 8 km) reported in some WR half grabens.
- Our models suggest that the faulting pattern observed in the upper crust can be (surprisingly) insensitive to variations in the vertical lithosphere strength distribution. While models with a single brittle layer (*a la Creme Brulee*) can produce hangingwall faulting patterns with appreciable similarity to WR basins, the inclusion of a 10 km thick, brittle mantle (model not shown) did not significantly change this pattern.
- The inclusion of a pre-existing optimally orientated fabric, in the models (dipping in both directions) significantly increases the tendency for models to generate dip domains, whereas when models are seeded with random noise, conjugate faulting patterns seem more prevalent.

References

[1] W. Bangerth, J. Dannberg, R. Gassmoeller, and T. Heister. Aspect v2.2.0, 2020.

[2] L. Moresi, F. Dufour, and H.-B. Mühlhaus. A lagrangian integration point finite element method for large deformation modeling of viscoelastic geomaterials. *Journal of computational physics*, 184(2):476–497, 2003.

[3] J.-A. Olive, M. D. Behn, E. Mittelstaedt, G. Ito, and B. Z. Klein. The role of elasticity in simulating long-term tectonic extension. *Geophysical Journal International*, 205(2):728–743, 2016.

[4] D. J. Shillington, C. A. Scholz, P. R. Chindandali, J. B. Gaherty, N. J. Accardo, E. Onyango, C. J. Ebinger, and A. A. Nyblade. Controls on rift faulting in the north basin of the malawi (nyasa) rift, east africa. *Tectonics*, 39(3):e2019TC005633, 2020.

[5] J. K. Weissel and G. D. Karner. Flexural uplift of rift flanks due to mechanical unloading of the lithosphere during extension. *Journal of Geophysical Research: Solid Earth*, 94(B10):13919–13950, 1989.

[6] L. J. Wright, J. D. Muirhead, and C. A. Scholz. Spatiotemporal variations in upper crustal extension across the different basement terranes of the lake tanganyika rift, east africa. *Tectonics*, 39(3):e2019TC006019, 2020.